Supporting Information

Kremkow et al. 10.1073/pnas.1310442111

SI Text

Supporting Information for Fig. 1. Thalamic neurons were recorded from the A layers of lateral geniculate nucleus (LGN; A and A1) within the region representing 5–20° of visual eccentricity. All thalamic neurons were classified as X or Y based on the linearity of spatial summation and as sustained or transient based on the transiency of their visual responses.

As demonstrated in Fig. 1 *C* and *D*, ON thalamic neurons had larger receptive fields in dark background than gray backgrounds. However, the receptive field size of OFF thalamic neurons was similar in light and gray backgrounds. This difference in receptive field size between ON and OFF thalamic neurons could be demonstrated in LGN cells classified based on linearity of spatial summation as X cells ($X\text{-}ON_{gray}/X\text{-}ON_{dark} = 0.63$, $P < 0.001$, $n = 31$; $X\text{-}OFF_{gray}/X\text{-}OFF_{light} = 1.03$, $P = 0.59$, $n = 41$) and Y cells ($Y\text{-}ON_{gray}/Y\text{-}ON_{dark} = 0.86$, $P = 0.012$, $n = 13$;$Y\text{-}OFF_{gray}/Y\text{-}OFF_{light} = 0.93$, $P = 0.46$, $n = 33$). It could also be demonstrated in LGN cells classified as sustained cells ($Sus\text{-}ON_{gray}/Sus\text{-}ON_{dark} = 0.68$, $P < 0.001$, $n = 31$; $Sus\text{-}OFF_{gray}/Sus\text{-}OFF_{light} = 1.03$, $P = 0.52$, $n = 39$) and transient cells ($Tran\text{-}ON_{gray}/Tran\text{-}ON_{dark} = 0.81$, $P = 0.014$, $n = 13$; $Tran\text{-}OFF_{gray}/Tran\text{-}OFF_{light} = 0.98$, $P = 0.43$, $n = 35$).

As demonstrated in Fig. 1 *A* and *B*, the receptive field size was larger in ON than OFF thalamic neurons when measured in light/dark background but not gray backgrounds. This result could be replicated if we restricted the sample to X cells (31 ON and 41 OFF) and sustained cells (31 ON and 39 OFF). ON X cells and ON sustained cells had larger receptive fields than OFF X cells and OFF sustained cells in dark/light backgrounds (X-ON/X-OFF: 1.68, $P < 0.0001$; Sus-ON/Sus-OFF: 1.68, $P < 0.0001$) but not gray backgrounds (X-ON/X-OFF: 1.08, $P = 0.144$; Sus-ON/Sus-OFF: 1.11, $P = 0.096$). The Y cells (13 ON and 33 OFF) and transient cells (13 ON and 35 OFF) showed a similar trend but did not reach significance probably because the sample was smaller (size ratios on light/dark backgrounds for Y-ON/Y-OFF: 1.08, $P = 0.078$ and Tran-ON/Tran-OFF: 1.16, $P = 0.197$; size ratios on gray backgrounds for Y-ON/Y-OFF: 1, $P = 0.616$ and Tran-ON/Tran-OFF: 0.96, $P = 0.201$).

Supporting Information for Fig. 2. The results from the rectified light and dark gratings showed a pronounced OFF dominance at low grating frequencies (Fig. 2). To further explore in what extent the V1 OFF dominance is spatial frequency dependent, we mapped receptive fields using randomized grating sequences and reverse correlation methods (1). This approach allowed us to precisely control the spatial frequency content of the stimulus (Fig. S1*A*). The grating sequences covered the full parameter space of 30 orientations, 30 spatial frequencies, and 4 phases and thus a total of 3,600 different gratings (stimulus update = 60 Hz, monitor refresh rate = 120 Hz). We tested three spatial frequency ranges: full = 0.03–0.75 cpd, mid = 0.06–0.75 cpd, and high = 0.12–0.75 cpd. The range of orientations and phases was fixed (orientation range = 0–180°, phase range = 0–180°). Fig. S1*B* shows receptive field maps of V1 sites that were simultaneously recorded with a linear multielectrode array probe that was inserted horizontally into cat V1 (interelectrode distance = 100 μm). When stimulated with the grating sequence containing the full spatial frequency range (0.03–0.75 cpd), the majority of the 32 available V1 recording sites could be mapped and were OFF dominated (Fig. S1*B*, bottom row). Increasing the lower bound of the spatial frequency range from 0.03 to 0.06 cpd, thus removing low spatial frequencies from the grating sequence, reduced the number of cortical channels that could be mapped and reduced the OFF dominance (Fig. S1*B*, middle row). Increasing the lower bound even further from 0.06 to 0.12 cpd, reduced even more the number of cortical channels that could be mapped and the OFF dominance (Fig. S1*B*, top row). Therefore, as we removed the low spatial frequencies from the stimulus, the cortical spread was reduced from 25 ± 4 recording sites with receptive field maps to 4 ± 4 (Fig. S1*C*). Moreover, as we removed the low spatial frequencies, the percentage of OFF-dominated sites decreased from 98% to 68% and the percentage of ON-dominated sites increased from 2% to 32% (Fig. S1*D*). If we normalize the receptive fields by the maximum absolute amplitude across all three spatial frequency ranges studied, the OFF signal strength decreased by ∼40% when low spatial frequencies were removed, whereas the ON signal strength remained relatively constant. These results demonstrate that the OFF dominance in V1 is spatial frequency dependent, a finding that can be fully explained by a model that uses the differences in the V1 luminance/response functions measured on gray backgrounds (*Supporting Information for Fig. 6*). The relative strengths of ON and OFF signals also depended on the grating contrast. To investigate this dependency, we selected 31 cortical sites that showed pronounced changes in the relative ON/OFF strength with contrast. We then classified these sites as ON dominated and OFF dominated (i.e., ON response stronger than OFF response for ON-dominated and vice versa for OFF-dominated). At 100% contrast, most of the 31 cortical sites were OFF dominated ($n = 27$, 87%). However, the number was greatly reduced at 50% contrast ($n = 16$, 52%) and was very low 25% contrast ($n = 4$, 13%). Therefore, 87% of the 31 cortical sites studied were OFF-dominated at high contrast but ON-dominated at low contrast.

Supporting Information for Fig. 5. To characterize the luminance/suppression function of lights and darks in LGN, we made use of the suppressive nature of the LGN receptive field surround. We first carefully estimated the position of the receptive field center using white noise. Then, we measured the optimal stimulus size by presenting circular stimuli of varying sizes on the receptive field center. We then covered the receptive field center with a high-contrast stimulus of optimal size and simultaneously stimulated the receptive field surround with an annulus of varying luminance. Both the center and surround stimulus were presented for 100 ms following a 150-ms pause on a gray background. We used light stimuli in ON-center cells and dark stimuli in OFF-center cells. We measured the luminance/suppression function for lights in ON-center cells (Fig. S2*A*) and for darks in OFF-center cells (Fig. S2*B*). Consistent with the differences of the luminance/response functions for lights and darks (Figs. 3 and 5), the luminance/suppression functions for lights had lower half saturation values (S_{50}) than the luminance/suppression functions for darks (average S_{50} lights = 0.39, S_{50} darks = 0.6, $P < 0.001$; Fig. S2*C*).

Supporting Information for Fig. 6. ***Retinal mosaics.*** Although ON retinal ganglion cells (RGCs) have larger dendritic fields than OFF RGCs, the magnitude of the irradiation illusion and the differences between ON and OFF receptive field sizes are likely determined by the luminance/response nonlinearity and not the dendritic fields. First, the differences in ON and OFF dendritic fields are small in central retina (2), which is the part of the retina used to perceive the irradiation illusion. Second, the differences between ON and OFF dendritic fields are always the same, whereas the magnitude of the irradiation illusion and the difference between ON and OFF receptive field sizes become more

pronounced when the nonlinearity in the ON luminance/response function increases. In fact, when we compared responses measured in gray and dark/light backgrounds, the L50 ratio and receptive field size ratio were correlated in ON LGN cells (L_{50dark}/L_{50gray} vs. $RF_{size\text{-}dark}/RF_{size\text{-}gray}$, $r = -0.598$, $P = 0.008$) but not OFF LGN cells ($L_{50light}/L_{50gray}$ vs. $RF_{size\text{-}light}/RF_{size\text{-}gray}$, $r = 0.177$, $P = 0.243$). Measurements of receptive field size are known to be stimulus dependent (3) and, as shown in our Fig. 1 *A* and *B*, the ON-OFF differences in receptive field size in LGN and V1 are greatly reduced on gray backgrounds, mostly due to a reduction of ON receptive field size. Obviously, the anatomy is the same under different background conditions. Therefore, changes in luminance/response nonlinearity, not static dendritic fields, explain changes in receptive field sizes and the irradiation illusion.

To reinforce this point even further, we provide an example in which the LGN receptive field sizes within the cat area centralis are larger for OFF- than ON-center cells. Clearly, this cannot be explained by the dendritic fields, which are larger for ON than OFF RGCs. However, it can be easily explained from the differences in ON and OFF response linearity. As shown in Fig. 1, when using sparse noise on binary backgrounds as stimuli, the receptive field size was larger in ON-center than OFF-center LGN neurons. However, OFF-center receptive fields could be slightly larger than ON-center receptive fields when mapped with white noise (Fig. S3 *A*–*C*; OFF/ON = 1.1, $P < 0.01$; the receptive field size was measured at 20% of the maximum amplitude).

How can this be explained? The weak OFF dominance that we demonstrate in LGN provides a possible answer. It is well known that the receptive field surround is stronger in LGN than in the retina (4) and that the surround is more effectively stimulated by large stimuli (white noise checkerboards) than small spots (sparse noise). LGN center and surround can be modeled as 2D Gaussian functions (5), with the surround having a larger spatial extend and a smaller amplitude than the center (Fig. S3*D*). Subtracting the surround from the center gives rise to the classical center-surround receptive field of LGN neurons. In this model, the amplitude of the surround controls the size of the receptive field center (the stronger the surround the smaller the receptive field center). Therefore, if the LGN responses are slightly stronger to darks than lights, the amplitude of the receptive field center should be slightly larger in OFF-center than ON-center neurons, a difference that would make the OFF receptive field centers slightly broader than ON receptive field centers. Moreover, a stronger OFF surround than ON surround will make the ON center smaller because there will be greater subtraction of OFF surround from ON-center than ON surround from OFF-center. Interestingly, the reported OFF dominance in the LGN (OFF/ON = 1.3, $P = 0.02$) is enough to make OFF-center receptive fields ~1.2 times larger than ON-center receptive fields (Fig. S3*E*), a value that is very close to the experimental measures of 1.1.

Model. Here, we describe a model that uses an early compressive nonlinearity at the level of the photoreceptor to explain the different dark/light spatial asymmetries that we describe in the paper. The model has four main equations that we describe below.

i) The convolution in Eq. **S1** describes the retinal luminance distribution $L(x)$ of a stimulus $I(x)$ passed through the optical point-spread-function of the eye (PSF). The PSF is roughly Gaussian and transforms binary stimuli into gray levels and sharp edges into blurred edges. For simplicity, we use just one dimension in visual space (x)

$$L(x) = PSF(x) * I(x). \quad \textbf{[S1]}$$

ii) The nonlinear function in Eq. **S2** describes the response output of photoreceptors $P(x)$ for each retinal location. L_{50} is the luminance intensity of the stimulus that generates 50% of the response (half-saturation intensity), n is the exponent of the nonlinearity, and P_{max} is the maximum response. Based on our results in LGN and V1, we assume that changes in background illumination (bg) affect the L_{50} [$L_{50}(bg)$] and n [$n(bg)$] of the photoreceptor luminance-response function. For example, $n(bg)$ is close to 1 when the background illumination is high and it becomes >1 when the background illumination decreases. The result is that the function is more compressive on dark than light backgrounds. The parameter values used in the model closely reproduced our LGN and V1 measurements (n: 1.6–2, L_{50}: 0.01–0.5, P_{max}: 1–1.5, bg: 0–120 cd/m^2)

$$P(x) = -P_{max}\frac{L(x)^{n(bg)}}{L_{50}(bg) + L(x)^{n(bg)}}. \quad \textbf{[S2]}$$

iii) Eq. **S3** describes the response output of the bipolar cells (B_{ON} and B_{OFF}) for each x retinal location. Both types of bipolar cells rectify the photoreceptor input and the ON bipolar inverts it as well. As a result, B_{ON} responds to light increments and B_{OFF} responds to light decrements relative to the background (bg). Note that, after this equation, subsequent transformations for ON and OFF pathways are identical

$$B_{ON}(x) = \max[-(P(x) - P(bg)), 0] \quad \textbf{[S3]}$$

$$B_{OFF}(x) = \max[(P(x) - P(bg)), 0].$$

iv) Eq. **S4a** describes the responses of ON (G_{ON}) and OFF (G_{OFF}) retinal ganglion cells at every retinal location. The responses of each ON and OFF retinal ganglion cells are calculated as the convolution of the responses from bipolar cells (B_{ON} or B_{OFF}) and the synaptic dendritic field (SDF) of the retinal ganglion cell. The SDF is defined as the distribution of synaptic weights from the driving input to the cell (e.g., input from bipolar cells in retinal ganglion cells). The SDF is assumed to be Gaussian and does not change with the stimulus conditions

$$G_{ON}(x) = SDF(x) * B_{ON}(x) \quad \textbf{[S4a]}$$

$$G_{OFF}(x) = SDF(x) * B_{OFF}(x).$$

Below we show how instantiations of Eqs. **S1**–**S4** can be used to explain the irradiation illusion (Fig. S4), differences in grating frequency tuning (Fig. S5), and differences in receptive field sizes of ON and OFF retinal ganglion cells (Fig. S6). Note that the only nonlinearities in the model are the photoreceptor response compression in Eq. **S2** and the bipolar rectification in Eq. **S3.**

a) The irradiation illusion is measured by comparing the perceived sizes of white squares on black backgrounds to black squares on white backgrounds, where both squares are larger than the SDF of ganglion cells (Fig. S4*A*). Eq. **S1** optically

blurs the edges of the white and black squares equally. Eq. **S2** is more compressive on black than white backgrounds, and therefore it acts as a neuronal blur of the photoreceptor output, which is more pronounced for white squares than black squares. Note that what we call neuronal blur is very different from the optical blur in that it is not linear and changes with background illumination. Hence, after rectification by the bipolar cells (Eq. **S3**), the population of ON retinal ganglion cells activated by white squares is larger than the population of OFF retinal ganglion cells activated by black squares, and this difference is transmitted along the visual pathway (Eq. **S4a**). On a gray background, the photoreceptor response functions are more similar for increments and decrements (Fig. S4*B*), and therefore the spatial extent of ganglion cell activation is also more similar for white and black squares. Notice that the irradiation illusion is also not perceived on gray backgrounds.

b) Eq. **S4b** describes the frequency tuning of a retinal ganglion cell when measured with half-rectified sinusoidal light and dark gratings (Fig. S5). The response (R_{ON} and R_{OFF}) at each frequency (f) is calculated as the amplitude of the convolution between the SDF of the cell and its inputs driven by half-wave rectified light and dark sinusoidal gratings. An SDF modeled as a difference of Gaussians leads to band pass spatial frequency tuning. The peak response occurs at the frequency at which the rectified stimulus best fills the center of the receptive field. Because of the greater neural blur, the peak ON stimulus will correspond to a higher physical frequency than the peak OFF stimulus, even if ON and OFF receptive fields have similar widths

$$R_{ON}(f) = Amp[SDF(x) * B_{ON}(L(\sin fx))] \qquad \textbf{[S4b]}$$

$$R_{OFF}(f) = Amp[SDF(x) * B_{OFF}L(\sin fx))].$$

c) The receptive field of a ganglion cell, $G(x)$, is measured as the spatial profile of responses to sparse stimulus impulses $S(x)$, which are smaller than the SDF (Fig. S6). The stimulus impulses are flashed at all retinal positions, x, that cover the SDF (Eq. **S4c**). Because the nonlinearity in Eq. **S2** depends on the background adaptation level, the spatial spread of bipolar cell activation by each stimulus impulse also depends on the stimulus conditions. For each impulse location, x, the spatial spread of the bipolar cell activation is broader for white impulses on black backgrounds than black impulses on white backgrounds. Consequently, the ganglion cell receptive field's width, given by the convolution of the fixed SDF with the bipolar response profiles, will be broader for ON than OFF retinal ganglion cells, even if the SDFs are similar for the two channels (notice that the dendritic fields of ON and OFF retinal ganglion cells are similar in central retina). Consistent with our results, these differences in receptive field size are strongly reduced on a midgray background because the response function is similar for increments and decrements

$$G_{ON}(x) = SDF(x) * B_{ON}(S(x)) \qquad \textbf{[S4c]}$$

$$G_{OFF}(x) = SDF(x) * B_{OFF}(S(x)).$$

We would like to emphasize that the compressive nonlinearity is similar for darks and lights when presented on gray backgrounds and more pronounced for lights on dark backgrounds than darks on light backgrounds. No background condition can make the nonlinearity more pronounced for darks. Therefore, across a wide range on backgrounds, lights are going to be more blurred than darks and the values of their receptive field sizes and peak grating frequencies are going to be also larger for lights. Finally, the model predicts that, if rectified dark and light half-wave gratings are distorted with an exponential nonlinearity of appropriate magnitude and sign, the cortical peak frequency should be higher for darks than lights. This prediction was also confirmed by our experimental results (Fig. S7).

SI Materials and Methods. ***Visual stimuli and receptive field analysis.*** Visual stimuli were generated in MatLab (The MathWorks) using the Psychophysics Toolbox extensions (6) and presented on a calibrated cathode ray tube monitor (cat: refresh rate = 120 Hz, mean luminance = 61 cd/m^2; monkey: refresh rate = 160 Hz, mean luminance = 62 cd/m^2). Receptive fields of the single neurons in the LGN and the multiunit activity in V1 were mapped with sparse noise by reverse correlation [spike-triggered average (STA)] and smoothed with a cubic spline. The stimulus had a grid of 20 × 20 positions. At a given stimulus frame, one sparse noise target covered 2 × 2 positions (~3 × 3°). The sparse noise target was either light (120 cd/m^2) or dark (<2 cd/m^2) and presented on a gray background (61 cd/m^2) or binary background (dark background, <2 cd/m^2; light background, 120 cd/m^2). Each stimulus sequence contained 8,400 frames (stimulus update, 30 Hz; monitor refresh rate, 120 Hz). The receptive field size was estimated by counting the number of pixels that crossed a noise threshold of 40%. In both the LGN and V1, we selected receptive fields with a signal-to-noise larger than 8. The Wilcoxon rank sum test was used as the statistical test.

Orientation and grating frequency tuning of lights and darks. To estimate the orientation and grating frequency tuning of light/dark stimuli, we generated static sinusoidal gratings and subsequently truncated the dark/light component, i.e., the negative going half (lights) or positive going half (darks), to the value of mean gray (Fig. 2*A*). We tested a full parameter space of 8 orientations (equally spaced between 0 and 180°), 10 grating frequencies (0.03–0.75 cpd on a log scale), and 4 phases for both light and dark gratings. The static gratings were presented for 100 ms, followed by a period of 200-ms mean gray. To estimate the tuning properties, we collected the spikes during the stimulus presentation (0–100 ms after stimulus onset) for each parameter combination. To reduce the 3D parameter space (orientation, grating frequency, phase), we summed across all phases, resulting in orientation/grating frequency responses maps for light and dark gratings (Fig. 2*B*). To estimate the orientation tuning properties, we selected the responses at the peak grating frequency and fitted the data with a Gaussian (Fig. 2*B*, horizontal white lines; Fig. 2*D*). From this fit, we extracted the orientation preference (the mean of the Gaussian) and the tuning bandwidth (half-width at half height). Likewise, the grating frequency tuning was estimated by fitting a Gaussian function to the responses at the preferred orientation (Fig. 2*B*, vertical white lines; Fig. 2*E*). From this fit, we characterized the grating frequency tuning by estimating the peak grating frequency (PF; Fig. 2 *E* and *G*) and the low frequency response (LFR), i.e., response at 0 cpd (Fig. 2 *E* and *H*). Only cortical sites with signal-to-noise larger than 2 and good fits ($R^2 > 0.6$) for all four tuning functions (orientation tuning for lights and darks, spatial frequency tuning for lights and darks) were included in the population analysis. Furthermore, we excluded cortical sites for which the fitted grating frequency tuning curve was outside of the tested frequency range, i.e., cortical sites with a high-frequency cutoff larger than 0.55 cpd were removed from the database.

Luminance/response functions for lights and darks.

Cat. To measure the luminance/response functions for lights and darks, we stimulated the neurons with a squared patch of ~3°/side positioned on the receptive field center. In V1, we used dark and light sparse noise to estimate the receptive field center, whereas

in the LGN, we used white noise to measure the receptive field center and sign (ON-center or OFF-center). The luminance of the patch was varied in 15 linear steps between dark (2 cd/m^2) and light (120 cd/m^2). The patch was presented for 100 ms followed by 100-ms background (dark = 2 cd/m^2, gray = 61 cd/m^2, light = 120 cd/m^2). We tested light increments on a dark background (ON-center cells in the LGN and V1 neurons), light decrements on a light background (OFF-center cells in the LGN and V1 neurons), and both light increments and decrements on a gray background. In the LGN, we tested each individual neuron with one square aligned with the receptive field center. In V1, we used grids of 3 × 3 or 4 × 4 squares to stimulate 32 recordings sites simultaneously. Only one square of the grid was presented at a given time, and we only included in the analysis recording sites with receptive fields completely covered by the grid. To calculate the luminance/response function in both LGN and V1, we counted the spikes during the stimulus presentation (0–100 ms) for each luminance value. The luminance/response measurements were fitted a Naka-Rushton function (7) to extract values of the maximum response (R_{max}) and half saturation (L_{50}: the luminance increment or decrement at which the responses reached half maximum). Only neurons that had a signal to noise larger than 2 and a good fit ($R^2 \geq 0.6$) were included in this population analysis.

Awake primate. The luminance/response functions were measured from responses of local field potentials to patches of ~2° centered on the receptive field. Here the luminance of the patch was varied in eight linear steps between dark (2 cd/m^2) and light (124 cd/m^2).

Human. The luminance/response functions were measured from visually evoked potentials to full-field checkerboards. The luminance of the "stimulus checkers" was varied in 11 linear steps between dark (2 cd/m^2) and light (124 cd/m^2), and depending on the condition, the "background checkers" were dark (2 cd/m^2), gray (62 cd/m^2), or light (124 cd/m^2).

1. Ringach DL, Sapiro G, Shapley R (1997) A subspace reverse-correlation technique for the study of visual neurons. *Vision Res* 37(17):2455–2464.
2. Dacey DM, Petersen MR (1992) Dendritic field size and morphology of midget and parasol ganglion cells of the human retina. *Proc Natl Acad Sci USA* 89(20):9666–9670.
3. Lesica NA, et al. (2007) Adaptation to stimulus contrast and correlations during natural visual stimulation. *Neuron* 55(3):479–491.
4. Hubel DH, Wiesel TN (1961) Integrative action in the cat's lateral geniculate body. *J Physiol* 155:385–398.
5. Cai D, DeAngelis GC, Freeman RD (1997) Spatiotemporal receptive field organization in the lateral geniculate nucleus of cats and kittens. *J Neurophysiol* 78(2):1045–1061.
6. Brainard DH (1997) The psychophysics toolbox. *Spat Vis* 10(4):433–436.
7. Naka KI, Rushton WA (1966) S-potentials from colour units in the retina of fish (Cyprinidae). *J Physiol* 185(3):536–555.

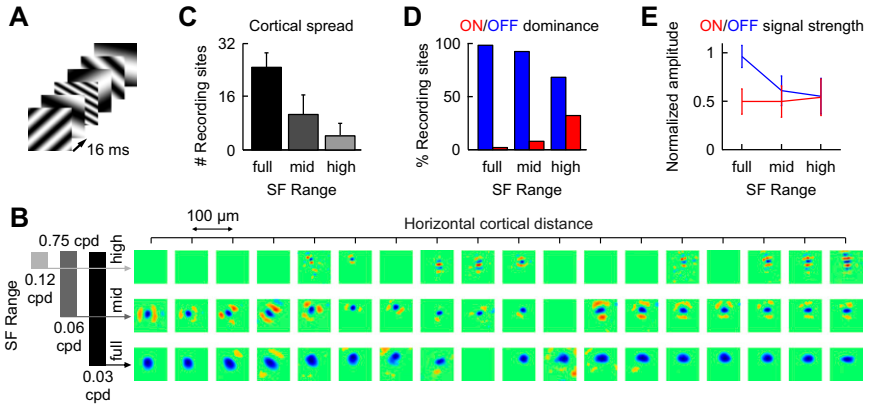

Fig. S1. Spatial frequency–dependent OFF dominance in V1. (*A*) Random grating sequence. (*B*) Spatial frequency–dependent receptive fields of 18 simultaneously recorded sites along a 1.7-mm-long horizontal track in V1 of cat using a linear multielectrode array probe (interelectrode distance = 100 µm; Neuronexus Inc.). When mapped with the full spatial frequency range (0.03–0.75 cpd, top row) almost all V1 recordings could be mapped and were OFF dominated. Removing low spatial frequencies (mid = 0.06–0.75 cpd or high = 0.12–0.75 cpd) reduced the number of V1 recordings that could be mapped. OFF, blue; ON, red. (*C*) The average cortical spread is very high when mapped with the full range, and it is greatly reduced when mapped with the high range. (*D*) Spatial frequency–dependent OFF dominance. (*E*) Spatial frequency–dependent signal strength.

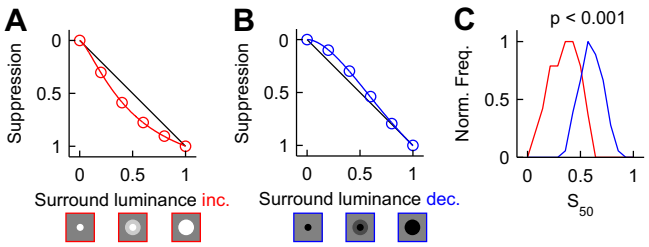

Fig. S2. Luminance/suppression functions of ON and OFF visual channels. (*A*) Luminance/suppression function of an ON-center LGN cell measured by driving the ON receptive field center with a light stimulus and simultaneously stimulating the suppressive ON surround with different luminance contrasts on a gray background. Half saturation of the suppression (S_{50}) was estimated from a Naka-Rushton fit. (*B*) Luminance/suppression function of an OFF-center LGN cell measured by driving the OFF receptive field center with a dark stimulus and simultaneously stimulating the suppressive OFF surround with different luminance contrasts on a gray background. (*C*) As for the luminance/response functions (Figs. 3 and 6), the luminance/suppression functions of lights have a lower half saturation than the luminance/suppression functions of darks.

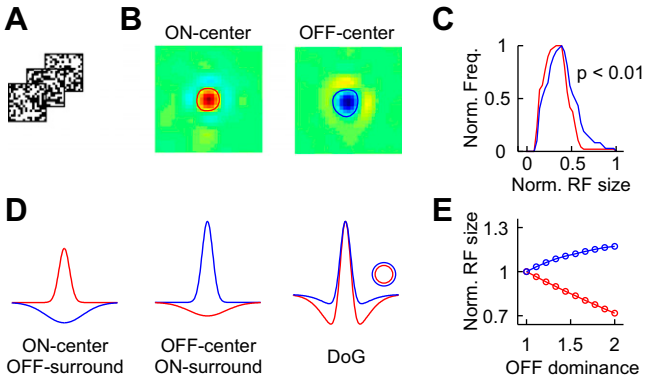

Fig. S3. Receptive field center size in the LGN measured with white noise. (*A*) White noise stimulus. (*B*) Example receptive fields of an ON-center and OFF-center LGN cell. The red and blue contours show the 20% threshold at which the center receptive field size was measured. (*C*) Distribution of ON-center (red) and OFF-center (blue) receptive field sizes. ON-center receptive fields are slightly but significantly smaller than OFF-center receptive fields when mapped with white noise. (*D*) Modified difference-of-Gaussian (DoG) model of ON-center (*Left*) and OFF-center (*Center*) LGN receptive fields with OFF dominance. Due to weak OFF dominance, ON-center receptive fields are smaller than OFF-center receptive fields (*Right*). (*E*) OFF dominance increases the OFF-center receptive field size (blue) and decreases the ON-center receptive field size (red).

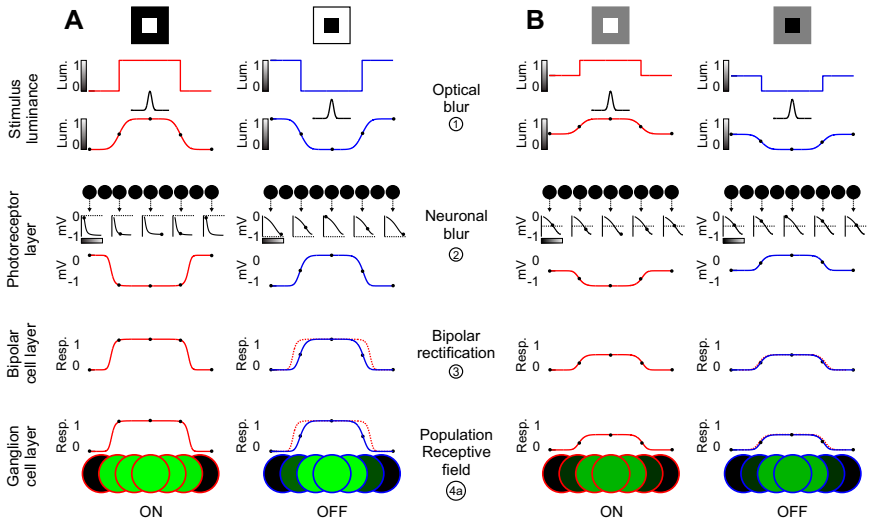

Fig. S4. A compressive nonlinearity in the photoreceptor can explain the irradiation illusion. (*A*) The irradiation illusion is measured by comparing the perceived sizes of white squares on black backgrounds to black squares on white backgrounds. (*A*, stimulus luminance) Any stimulus projected onto the retina is blurred by the optics of the eye (optical blur, Eq. **S1**). Note that the optical blur (Gaussian black line) is the same for light and dark stimuli. (*A*, photoreceptor layer) The response output of each photoreceptor (black circles, Eq. **S2**) also causes a spatial blur in the stimulus (neuronal blur). Because the photoreceptor response is more compressive on black than white backgrounds (luminance/response functions below the black circles), the neuronal blur is more pronounced for white squares than black squares. The luminance adaptation level of the photoreceptor is illustrated by horizontal dotted lines superimposed on the luminance response functions. (*A*, bipolar cell layer) The photoreceptor output is rectified by the bipolar cells (Eq. **S3**). The spatial blur is larger in ON bipolar cells (red line) than OFF bipolar cells (blue line). To facilitate the comparison, the spatial blur for ON bipolar cells is shown as a dotted line superimposed in the spatial blur for OFF bipolar cells. (*A*, ganglion cell layer) Because of the neuronal blur, white squares activate a larger population of retinal ganglion cells than black squares (Eq. **S4a**). (*B*) On gray backgrounds, the photoreceptor response functions are more similar for increments and decrements, and therefore the sizes of the activated ON and OFF cell populations are also similar. Note that irradiation illusion is not perceived in gray backgrounds.

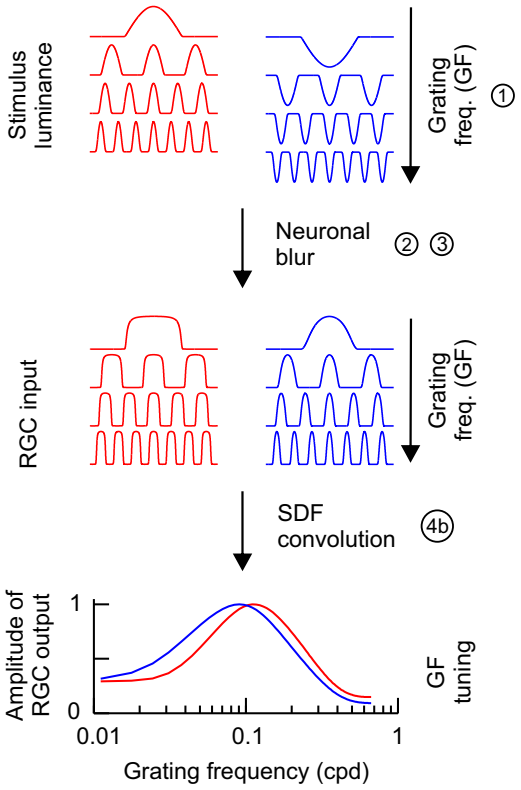

Fig. S5. A compressive nonlinearity in the photoreceptor can explain the differences in grating frequency tuning for lights and darks. (*Top*: stimulus luminance) Half-wave rectified light (red) and dark (blue) gratings have same grating frequency components after the optical blur (Eq. **S1**). (*Middle*: RGC input) The neuronal blur results in a broadening of the light rectified gratings at the level of the input to the retinal ganglion cells (RGC input, Eqs. **S2** and **S3**). (*Bottom*: amplitude of RGC output) Convolution between the light and dark rectified grating inputs and the synaptic dendritic field (SDF) of the retinal ganglion cell (Eq. **S4b**) results in the grating frequency tuning curves. The SDF is defined as the spatial distribution of the synapses from bipolar cells onto the dendritic field of the retinal ganglion cell. Due to the neuronal blur, the peak grating frequency is higher for light than dark half-wave rectified gratings.

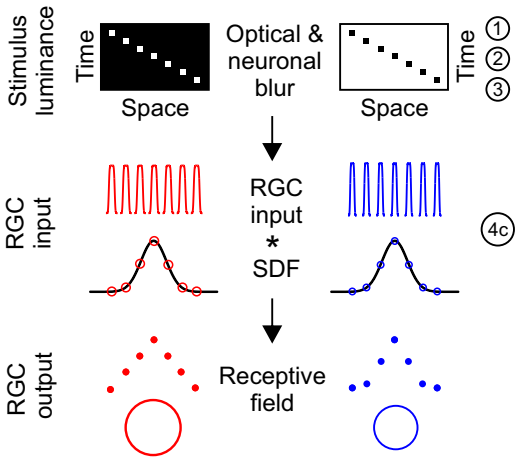

Fig. S6. A compressive nonlinearity in the photoreceptor can explain the differences in the receptive field sizes of ON and OFF RGCs. When sparse noise stimuli are used to measure a receptive field (*Top*), the optical blur is similar for light and dark spots (Eq. **S1**), but the neuronal blur is more pronounced for light spots (Eqs. **S2** and **S3**). The convolution of the RGC input with the SDF (*Middle*; Eq. **S4c**) results in larger receptive field maps for ON than OFF retinal ganglion cells (*Bottom*).

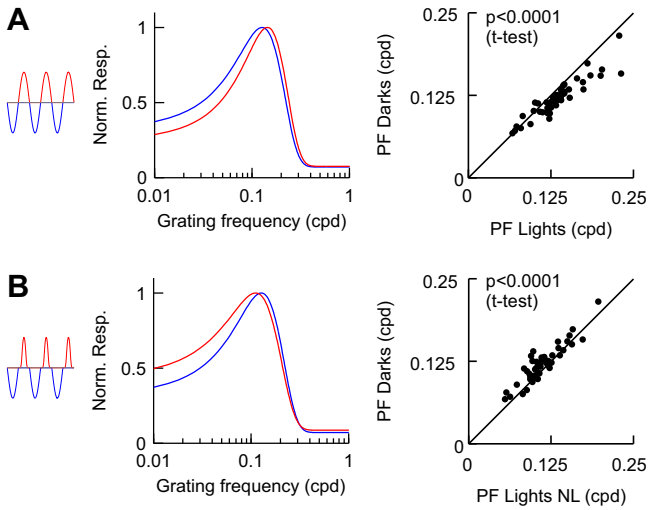

Fig. S7. Nonlinear encoding of stimuli on the monitor can counteract the neuronal blur. (*A*) Grating frequency tuning of V1 neurons to light and dark rectified sinusoidal gratings with linear encoding of the stimulus on the monitor (*Left*). Example V1 recording showing higher peak frequency for light than dark gratings (*Center*). When using linear encoding, most V1 recordings had higher peak frequencies for light than dark gratings ($n = 48$, average peak frequency is 1.12 times larger for lights than dark gratings). (*B*) Nonlinear encoding of the light stimulus on the monitor (*Left*) counteracts the neuronal blur and results in higher peak frequency of dark than light gratings (*Center* and *Right*, $n = 48$, average peak frequency is 1.12 times larger for darks than lights).